APPLICATION OF HOLOGRAPHIC INTERFEROMETRY TO ANALYSIS OF SINUSOIDALLY-EXCITED ACOUSTIC TRANSDUCERS

David John Griffiths

United States
Naval Postgraduate School

THESIS

APPLICATION OF HOLOGRAPHIC INTERFEROMETRY
TO ANALYSIS OF SINUSOIDALLY-EXCITED
ACOUSTIC TRANSDUCERS

by

David John Griffiths

December 1969

Application of Holographic Interferometry to Analysis of Sinusoidally-excited Acoustic Transducers

by

David John Griffiths
Lieutenant, United States Navy
B.S., University of Washington, 1962

Submitted in partial fulfillment of the
requirements for the degree of

MASTER OF SCIENCE IN ENGINEERING ACOUSTICS

from the

NAVAL POSTGRADUATE SCHOOL
December 1969

ABSTRACT

An application of optical holography known as "Holographic Interferometry" has been developed which enables experimentalists either to measure deformations of a few microns in loaded mechanical systems or to examine relative displacements in sinusoidally-vibrating systems. The fundamental theory of holography and four techniques for holographic interferometry are described in this report. A system constructed to record interferograms of acoustic transducers operating either in air or submerged in water is discussed and some results of examining a sinusoidally-excited 7-inch permanent-magnet loudspeaker with interferograms are considered.

TABLE OF CONTENTS

I. INTRODUCTION

A hologram is a recording of a three-dimensional object which contains the information necessary to reconstruct an image of the object in three dimensions for viewing or photographing. The terms "hologram" and "holography" were coined by Dr. D. Gabor in 1948 [1].

Early investigations of holography examined the process itself, but little practical application was made of the process until the 1960's. In more recent years a technique called "holographic interferometry" has been employed to observe static and dynamic deformation of mechanical systems under influence of stress or vibration. Currently, four different techniques have been developed for holographic interferometry. Each of these techniques, while having particular advantages for specific applications, have certain common advantages; primary among these are (1) there is no physical "loading" of the system under examination with unwanted masses, (2) amplitude of vibrations of a few microns can be observed, (3) frequency of the vibrations is unimportant insofar as the holographic process is concerned, and (4) the system under test can be examined without destruction.

The application of holographic interferometry to acoustical transducers is obvious. Sinusoidally-excited devices of complex geometry can be investigated either to determine displacements

and velocities in order to compare mathematical models with experimental results, or to aid in construction and design where mathematical modeling is not readily attainable.

This report deals with descriptions of the four techniques of holographic interferometry, experimental apparatus used to record time-averaged vibration interferograms, and some experimental results.

II. HOLOGRAPHIC INTERFEROMETRY

A. THEORY

1. Hologram Recording

The relevant features of the holographic technique are illustrated in Fig. 1 [1]. The light scattered from the object has some spatially dependent amplitude function $A(x)$ and spatially dependent phase function $\phi(x)$ at the plane of the photographic plate. The reference beam incident on the plate from the prism is assumed to have uniform amplitude A_0 and a phase function of the form $\phi_r(x) = -\alpha x$. The constant α relates the angle θ and the wavelength according to the equation

$$\alpha\lambda = 2\pi \sin\theta \qquad \text{II.1}$$

which for small angles can be written

$$\alpha \doteq \frac{2\pi\theta}{\lambda} . \qquad \text{II.2}$$

Thus, by superposition, the amplitude at the photographic plate is

$$A_0 \exp[-i\alpha x] + A(x) \exp[i\phi(x)]. \qquad \text{II.3}$$

(The time variation $e^{-i\omega t}$ of the light source is to be understood in this development.) The intensity of this incident beam is

$$\begin{aligned} I(x) &= \left\{ A_0 \exp[-i\alpha x] + A(x)\exp[i\phi(x)] \right\} \cdot \\ &\quad \left\{ A_0 \exp[i\alpha x] + A(x)\exp[-i\phi(x)] \right\} \qquad \text{II.4} \\ I(x) &= A_0^2 + A(x)^2 + A_0 A(x) \left\{ \exp[i(\alpha x+\phi(x))] \right. \\ &\quad \left. + \exp[-i(\alpha x+\phi(x))] \right\} \end{aligned}$$

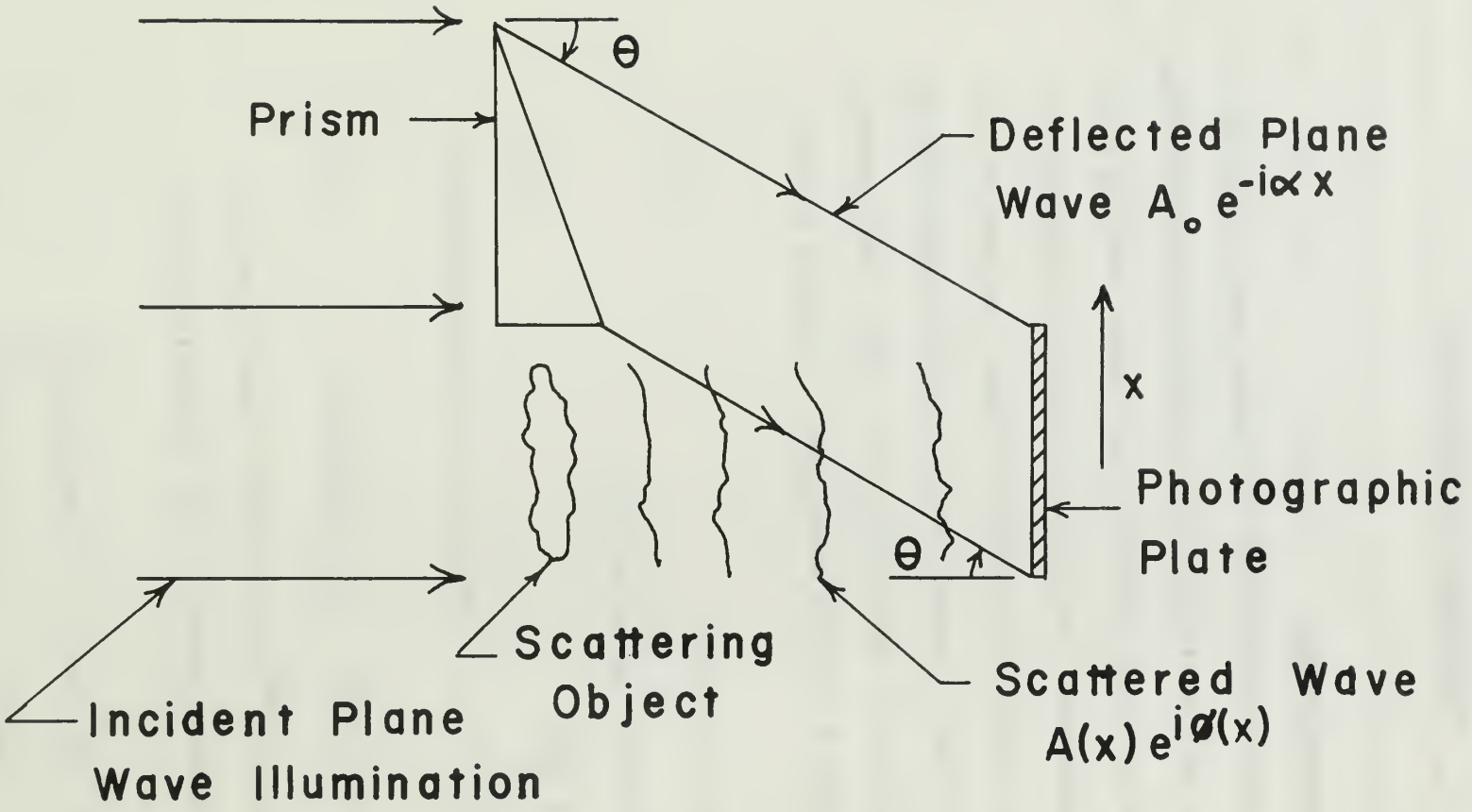

FIG. 1 HOLOGRAM CONSTRUCTION

The phase information $\phi(x)$ of the scattered wave has been retained in the intensity equation.

The photographic plate records some power of the intensity. This is best explained by the plate's "characteristic curve", a graph of silver density at a point on the plate versus the logarithm of exposure [2]. Exposure E is defined as the product of light intensity I and the time t of exposure. A representative characteristic curve is shown in Fig. 2 [2]. It can be seen that over a considerable region of the curve the density D is linearly related to the logarithm of exposure; i.e.,

$$D = \gamma \log E \qquad \text{II.5}$$

$$D = \log E^{\gamma}$$

where γ is the slope of the linear portion of the characteristic curve. Alternatively, the density D is defined as

$$D = \log \frac{1}{T} \qquad \text{II.6}$$

where T is the intensity transmission. Thus, combination of Eqs. II.5 and II.6 yields

$$T = E^{-\gamma}. \qquad \text{II.7}$$

Since it is desirable to deal with the amplitude of light transmitted by the processed hologram rather than light intensity, amplitude transmission T_a is defined as

$$T_a = T^{\frac{1}{2}} = E^{-\gamma/2}. \qquad \text{II.8}$$

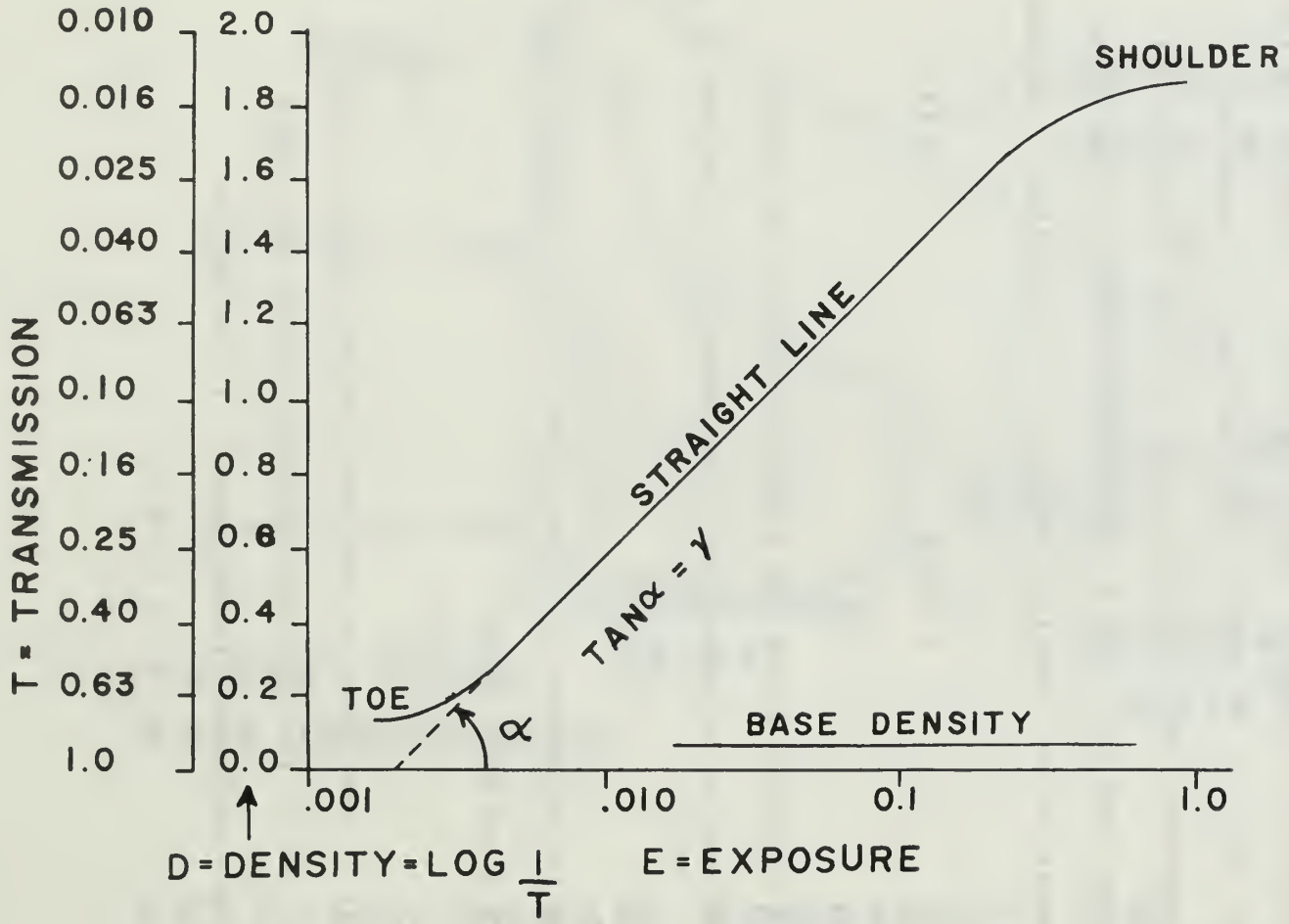

FIG. 2 EMULSION CHARACTERISTIC CURVE

Recalling that

$$E = It \qquad \text{II.9}$$

for a constant time t, we may combine Eqs. II.8 and II.9 to obtain

$$T_a \propto I^{-\gamma/2}. \qquad \text{II.10}$$

Thus, for a hologram constructed such that the exposure was made in the linear portion of the characteristic curve of the photographic plate, the transmitted amplitude $T_a(x)$ of the processed hologram is

$$T_a(x) \propto [I(x)]^{-\gamma/2}. \qquad \text{II.11}$$

Expanding Eq. II.11 in terms of Eq. II.4 reveals

$$T_a(x) \propto \left\{A_0^2 + A^2(x) + A_0A(x)\left[\exp[i(\alpha x + \phi(x))] + \exp[-i(\alpha x + \phi(x))]\right]\right\}^{-\gamma/2} \qquad \text{II.12}$$

$$T_a(x) \propto (s_0 + s)^{-\gamma/2}$$

where

$$s_0 = A_0^2 + A^2(x) \qquad \text{II.12a}$$

and

$$s = A_0A(x)\left\{\exp[i(\alpha x + \phi(x))] + \exp[-i(\alpha x + \phi(x))]\right\}. \qquad \text{II.12b}$$

If Eq. II.12 is expanded in a Binomial series, we have

$$T_a(x) \propto s_0^{-\gamma/2}\left[1 - \gamma/2(s/s_0) + \frac{(\gamma/2)(\gamma/2+1)}{2!}\left(\frac{s}{s_0}\right)^2 + \cdots + (-1)^n \frac{(\gamma/2+1)\cdots(\gamma/2+n-1)}{n!}\left(\frac{s}{s_0}\right)^n + \cdots\right]. \qquad \text{II.13}$$

If $\frac{s}{s_0} \ll 1$, higher order terms containing $\left(\frac{s}{s_0}\right)^n$ may be dropped, which yields the approximation

$$T_a(x) \propto s_0^{-\gamma/2} - \gamma/2\, s_0^{-\gamma/2-1}\, s. \qquad \text{II.14}$$

This can be rewritten as [3]

$$T_a(x) \propto A + Bs \qquad \text{II.15}$$

where $A = s_0^{-\gamma/2}$ and $B = \gamma/2 s_0^{-\gamma/2-1}$.

2. Reconstruction

If the processed holograph is illuminated by a plane wave of monochromatic light A_1 of the same frequency as the light used in the construction, a wave A_2 modulated by the holograph, is produced

$$A_2 = A_1(A + Bs). \qquad \text{II.16}$$

Considering only the s term in Eq. II.16 expanded in terms of II.12b

$$A_2 \propto A_1 A_0 A(x) \left\{\exp[i(\alpha x+\phi(x))] + \exp[-i(\alpha x+\phi(x))]\right\}. \qquad \text{II.17}$$

Results of modulating the incident plane wave A_1 are illustrated in Fig. 3. The two images are generated by the terms of Eq. II.17: (1) The real image is a result of the first term $A_1 A_0 A(x)\exp[i(\alpha x+\phi(x))]$; since it occurs in front of the holograph, it can be projected on a screen placed at the position of the image. (2) The virtual image is a result of the second term $A_1 A_0 A(x)\exp[-(\alpha x+\phi(X))]$; recalling that the time variation $e^{-i\omega t}$ has been dropped in this development

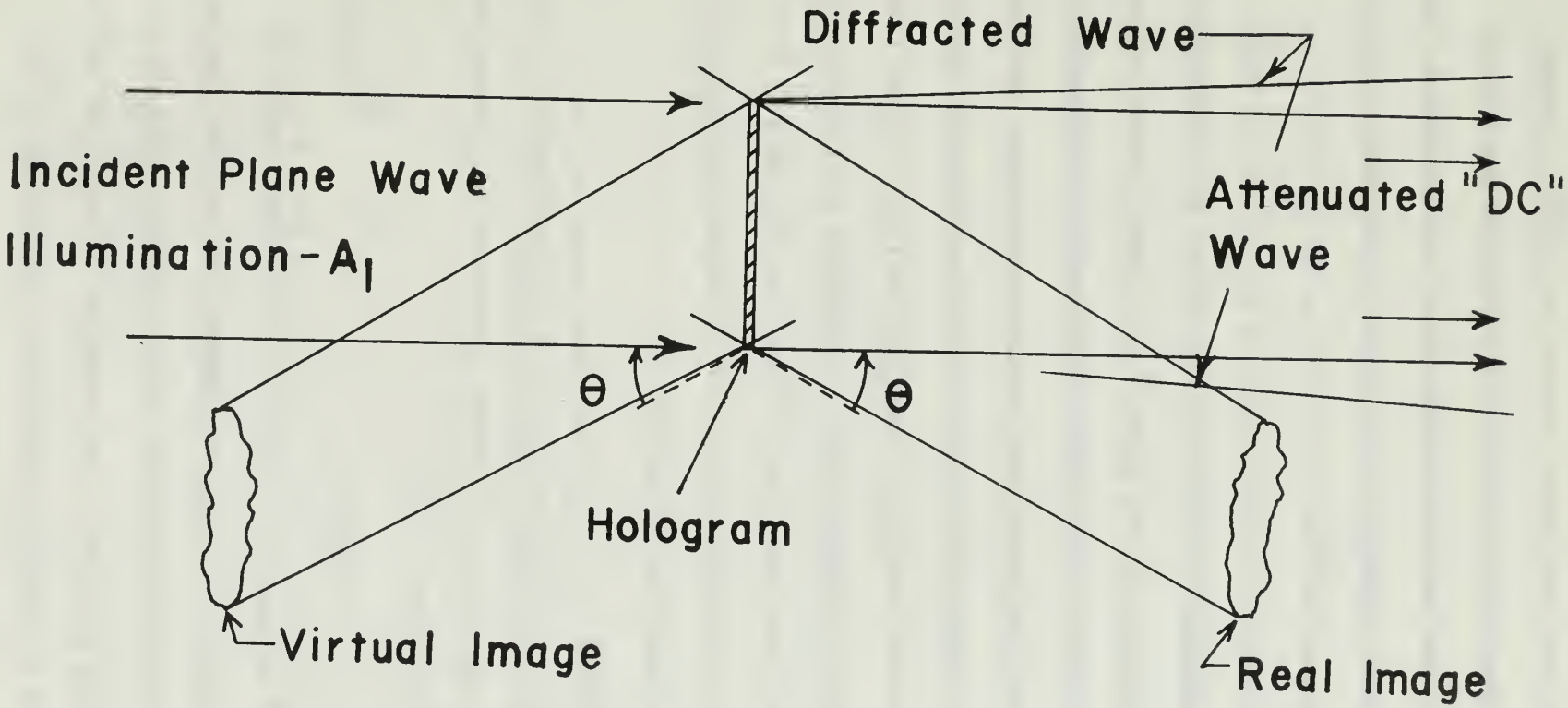

FIG. 3 HOLOGRAM RECONSTRUCTION

it can be seen that the phase information $e^{-\phi(x)}$ travels "backwards in time" generating a virtual image behind the holograph which can be viewed directly or photographed. Both images are shifted from the axis of the illuminating wavefront by the linear phase $e^{\pm i\alpha x}$.

So far only the second term of Eq. II.16 has been considered. Expanded in terms of Eq. II.12a Eq. II.16 yields terms in A_2 proportional to $A_0^2 + A^2(x)$. These terms contain amplitude information only. The first term is analogous to a direct-current component of a modulated voltage. The second term describes density variations in the emulsion of the processed plate which results in some diffraction of the illuminating wavefront. However, A(x) is normally a slowly varying function. Thus, the resulting diffraction is small. Both terms indicate an attenuation of the illuminating plane wave when passed through the holograph.

3. Resolution

For the two waves incident on the photographic plate in Fig. 1 the separation d between interference fringes recorded in the emulsion is [4]

$$d = \frac{\lambda}{\sin \theta} . \qquad \text{II.18}$$

As the angle θ between the reference and object beams increases the separation between interference fringes decreases. This places a major requirement on the resolving capability of the recording emulsion. For example, an angle of 20° and a wavelength of 0.6 microns requires a resolution of 540 fringes/mm.

4. Coherence Length

The foregoing theory is based on the assumption of a perfectly monochromatic light source. Since this cannot be realized physically it is necessary to examine the limitations of a light source whose spectral distribution has some finite width [1].

Two waves of frequency f and $(f-\Delta f)$ describe the center frequency f and the frequency $(f-\Delta f)$ at the lower extreme of a light source with finite spectral width $2\Delta f$. If at some time $t = 0$ the two frequencies are in phase then at some later time t the phase difference between the two frequencies is

$$\Delta\phi = 2\pi ft - 2\pi(f-\Delta f)t = 2\pi t\Delta f. \qquad \text{II.19}$$

During this same time the two waves travel a distance

$$L = ct. \qquad \text{II.20}$$

The relationship

$$c = f\lambda, \qquad \text{II.21}$$

where c is the free space speed of light and λ the wavelength of the light frequency f, when differentiated with respect to λ yields

$$\frac{df}{d\lambda} = -\frac{c}{\lambda^2} \qquad \text{II.22a}$$

$$\Delta f \doteq -\frac{c}{\lambda^2}\Delta\lambda. \qquad \text{II.22b}$$

A combination of II.19 and II.22b yields

$$\Delta\phi \doteq -2\pi\frac{\Delta\lambda}{\lambda^2}ct. \qquad \text{II.23}$$

If coherence length L_c is defined as the length L for which the two frequencies are out of phase by $\frac{\pi}{2}$ then combination of Eqs. II.20 and II.23 results in

$$L_c = \frac{1}{4}\frac{\lambda^2}{\Delta\lambda} . \qquad \text{II.24}$$

From Eq. II.24, we see that if the difference in length traveled by the reference beam and the length traveled by the object beam in Fig. 1 is equal to L_c, the contrast in the interference fringes recorded by the photographic plate would be approximately half that which would be recorded if there were no difference in path lengths. Coherence length also imposes a limitation on the depth a given object can extend and still be successfully reconstructed in a hologram. A difference in path lengths greater than the coherence length L_c would result in greater loss in fringe contrast as the difference increased, eventually resulting in a failure of the holographic process.

B. METHODS OF HOLOGRAPHIC INTERFEROMETRY

1. Static Deformation Interferograms

Analysis of statically-deformed systems can be made holographically by the following double exposure technique: The system under examination is first holographed without the influence of the deforming stress. Then, without disturbing the photographic plate, the device is loaded and a second exposure made. The processed and reconstructed hologram will display the two slightly different images superimposed.

Where the phases of the two images add constructively the viewed image will be bright. Conversely, where the images are out of phase by one-half the wavelength of the illuminating light the image will be dark. If a point of reference on the object known to remain fixed under load and noload conditions is established in the observed system the relative displacement of the object can be determined and the deformation fringes read like a contour map.

Fringing is a function of the geometry of the hologram recording and reconstruction systems. Figure 4 illustrates this dependence. A point P_1 is illuminated during the recording process with a plane wave which forms an angle ϕ_1 with a normal to the object at P_1 and a first exposure is made. A second exposure is made after a static load is applied moving point P_1 through a distance ∂ to point P_1'. If ∂ is assumed small compared to distances ℓ_1 and ℓ_1', then ϕ_1 does not change appreciably. During reconstruction the two slightly different images are observed at a point 0 which forms an angle ϕ_2 with a normal to the object at points P_1 and P_1'. The apparent distances light travels from the source through the points P_1 and P_1' to 0 are $\ell_1 + \ell_2$ and $\ell_1' + \ell_2'$ respectively. If destructive interference between the two images is assumed the paths difference must be

$$(\ell_1 + \ell_2) - (\ell_1' + \ell_2') = (2n-1)\frac{\lambda}{2}; \quad n = 1,2,3.... \qquad \text{II.25}$$

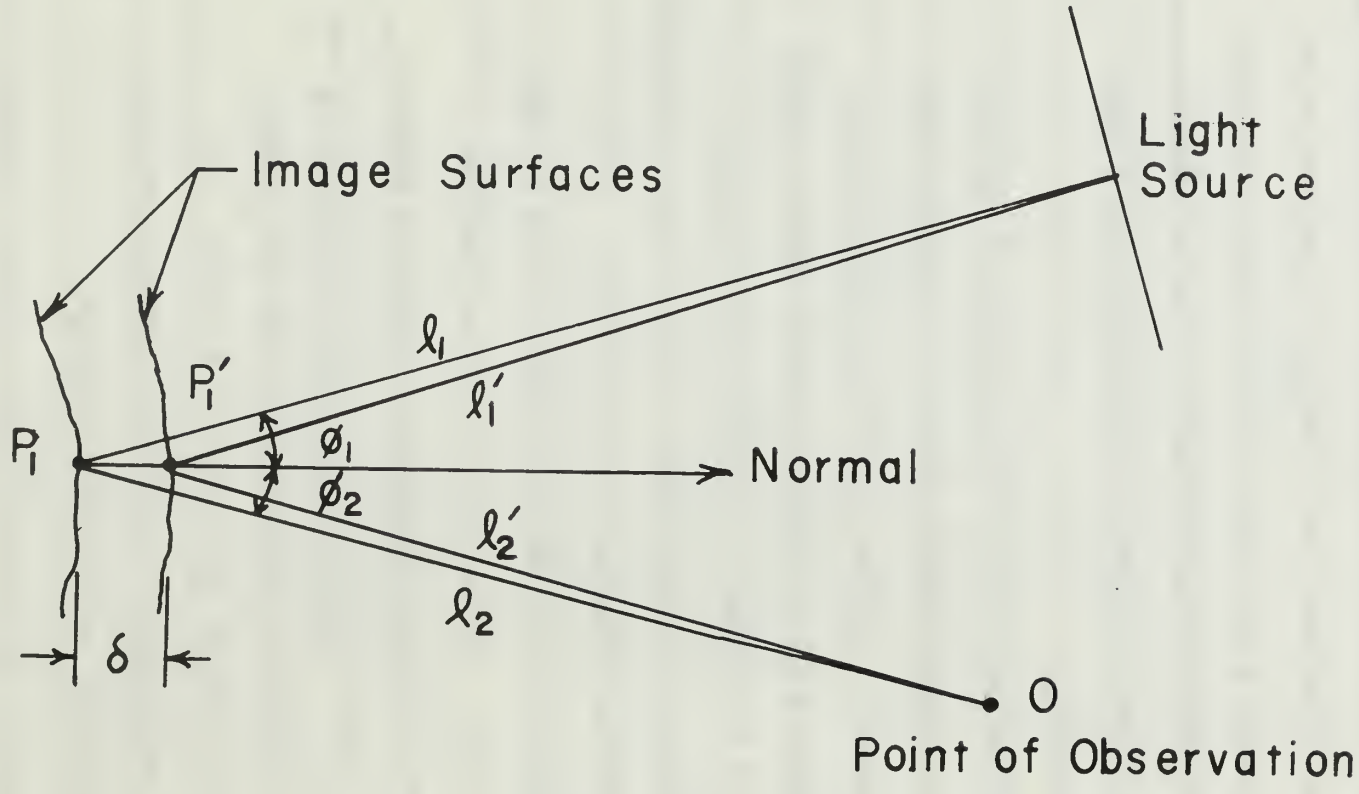

FIG. 4 STATIC DEFORMATION INTERFEROGRAM
INTERFERENCE-FRINGE GEOMETRY

but,

$$\ell_1' = \ell_1 - \partial \cos \phi_1$$

and,

$$\ell_2' = \ell_2 - \partial \cos \phi_2$$

thus, Eq. II.25 reduces to

$$\partial(\cos \phi_1 + \cos \phi_2) = (2n-1)\frac{\lambda}{2} . \qquad \text{II.26}$$

Therefore, the deformation distance at dark fringes of the image can be computed with knowledge of the angles ϕ_1 and ϕ_2 and the light wavelength.

More precisely, provided the displacement is sufficient, a first-order dark fringe (n = 1) will appear adjacent to the fixed reference point on the object. Second, third, and higher order fringes will appear successively removed from the reference point. These dark fringes will be separated from each other by bright fringes where the two images add constructively.

2. Time-averaged Vibration Interferograms

Interferograms of a vibrating device can be made with a single exposure of the object. The reconstructed image from the interferogram will record a very large number of fringe patterns. Since the action of the film emulsion is to integrate the images, the reconstructed pattern will be related to the probability density function of the amplitude of vibration. Thus, for a sinusoidally-vibrating device the time-averaged hologram will contain information primarily related to the displacement at the positive and negative peaks of excursion. Nodal positions of the vibrating object will be indicated by maximum intensity in the reconstructed image.

Fringes for sinusoidal vibration are predicted by [5]

$$\frac{I}{I_{ST}} = J_0^2 \left[\frac{2\pi}{\lambda} (\cos \phi_1 + \cos \phi_2)\partial\right] \qquad \text{II.27}$$

where I is the intensity of the image, I_{ST} the intensity the stationary image would have, ϕ_1 the angle between the object beam and the normal to the object surface, ϕ_2 the angle between the axis of observation and the normal to the object surface, λ the wavelength of the light source, and ∂ the displacement. $J_0^2(\xi)$ is maximum when the displacement ∂ is zero; thus, nodal lines are easily recognizable in the reconstructed hologram. The zeros of $J_0^2(\xi)$ occur at $\xi_n = 2.405, 5.52$, etc.. Hence, the displacement where dark fringes occur can be calculated by setting the argument of Eq. II.27 equal to the numerical values of ξ_n and solving.

As in a static-deformation interferogram, the order and number of fringes can be referred to a known fixed position on the object. Here, however, the first dark fringe adjacent to the reference point corresponds to the first zero of $J_0^2(\xi)$, the second dark fringe to the second zero and so on.

3. Stroboscopic Interferograms

A third possibility exists for interferometric holography [6]. An exposure of the stationary object can be made and then a second exposure on the same film made of the object in motion by illuminating the object only during a small increment of the period of the vibration. The light

source is synchronized to illuminate the object for the same small increment of each vibration cycle over many cycles. This is most readily attainable by use of a Kerr or Pockels-cell shutter synchronized to the desired vibration increment. The resulting interferogram will be related to the displacement of the selected increment only, rather than a statistical average. Holograms of successive increments over the complete vibration cycle can be used to determine the velocity of the vibrating object.

4. Real-Time Interferograms

Finally, if it is desired to observe deformation or vibration in real time a hologram can be made of the object in a static, unloaded condition. The photographic plate is then processed and repositioned exactly as before exposure, the object strained or excited, and the resulting fringes observed. While this technique sounds reasonable, in practice it is the most difficult of all in that the developed plate must be precisely repositioned--not an easy task. Additionally, the chemical removal of unexposed silver halides in the development of the photographic plate causes a shrinking of the emulsion which results in some exterraneous fringing even when the holograph is perfectly repositioned. This can be reduced by further chemical processing, but this in itself requires great care. In cases of real-time observation of vibrating objects a few static fringes due to imperfect realignment or emulsion shrinkage are desirable [7]. The eye

would be unable to integrate the rapidly changing interfering images as does a photographic plate; however, motion can be deduced from the washing out of static fringes where the object is in motion, or the persistance of static fringes where nodal positions occur on the vibrating object.

III. EXPERIMENT

A. EXPERIMENTAL CONSIDERATIONS

For successful holography a number of requirements must be met. First a source of coherent, monochromatic light is needed. This is dictated by the requirement of a spatially-coherent reference beam and the limitations imposed by the coherence length for the source. Secondly, the slow speed of high-resolution emulsions and low intensities of the reference and object beams often lead to long time-exposures in the recording process. This coupled with the interference-fringe separations on the order of a few microns demands that the recording system be in thermal and mechanical equilibrium and essentially insensitive to external vibration.

The resolution of the recording emulsion must be compatible with the interference fringe separations resulting from the geometry of the recording system. For most holography high-resolution emulsions must be employed. Although standard darkroom techniques will usually suffice to produce adequate holograms, it must be remembered that any change in the recording emulsion after exposure will result in distortion of the reconstructed image. Consequently, extreme care should be exercised in the processing and handling of holograms.

B. HOLOGRAPHIC EQUIPMENT AND ARRANGEMENT

The experimental apparatus was arranged so that interferograms of objects in air and water could be made. While the system demonstrated successfully that it could produce adequate holograms of transducers submerged in water, transducers were not readily available capable of producing sufficient sound pressure levels and associated displacements for adequate fringing [8]. Consequently, only objects driven in air were investigated.

The light source was a Model 116 Spectra-Physics, He-Ne CW laser. The laser's nominal power output was twenty-five milliwatts for single-mode operation at 6328$\mathring{A}$ wavelength. Additional equipment required included

(a) spatial filters

(b) front-surfaced optical mirrors

(c) negative lenses

(d) optical-glass windows

(e) beam splitter

(f) KODAK Type 649F High-resolution Spectroscopic Plates

(g) KODAK D-19 High-contrast Developer

(h) stop bath, fixer, and associated darkroom equipment.

The peculiar geometry and location of the holographic recording equipment made using the Model 116 laser convenient for reconstructing the interferograms. Accordingly, a Gaertner-Jeong Holographic System [4] was employed for reconstruction.

Figure 5 illustrates the arrangement of the equipment used for the hologram recording process. The base consisted of a 10' x 6' x 2' plywood box. The box was filled to approximately a one foot depth with dry sand. Then a 8' x 4' x 3' steel tank was centered in the half-filled box and the remaining void filled with sand. This left approximately two feet of the tank extending above the sand. The exposed sand was covered with plywood which served to support the external optical equipment. Care was exercised in the construction to avoid allowing the plywood top to contact the tank. It was thought that this would reduce external vibrations from being transmitted to the tank through the plywood. Additionally no voids between the plywood and the sand were allowed in an effort to dampen vibrations which might have occurred in the plywood. Approximately three-and-a-half tons of dry sand were used to provide mechanical stability and damping in the system.

Parallel-sided optical-glass windows were placed in the side of the tank, and the optical equipment was arranged to provide the reference beam and object-illuminating beam as shown in Fig. 5.

The He-Ne laser was mounted on a bench external of the tank and base. Theory requires only that the light from the reference and object beams be coherent; thus, small vibrations in the light beam before the beam splitter can be tolerated. Therefore, the laser did not require the rigid stability of the other components positioned after the beam splitter. The

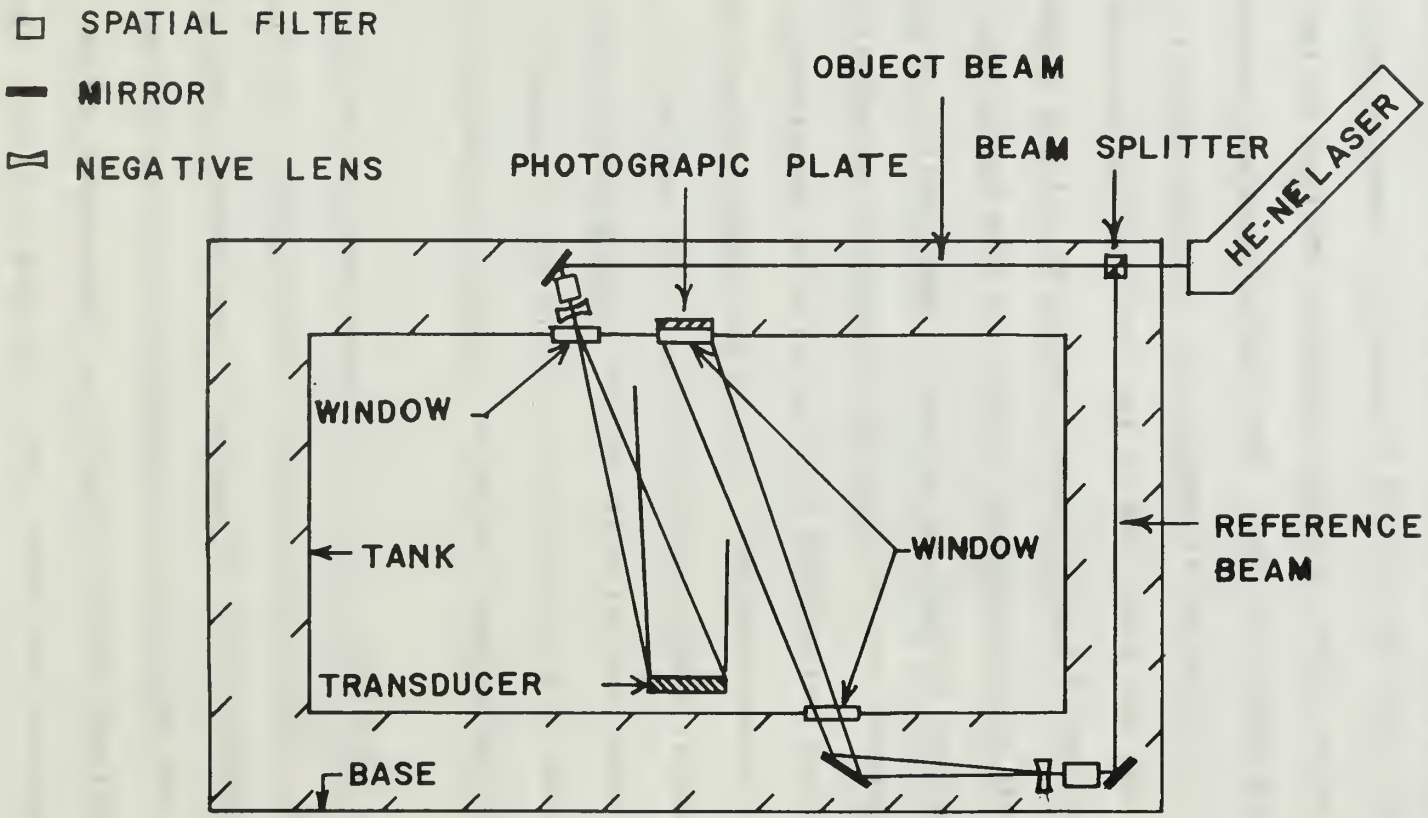

FIG. 5 HOLOGRAPH RECORDING SYSTEM

mounts for optical equipment were made of heavy block masses to reduce their being influenced by air-carried vibrations and were secured in place after alignment.

Acoustical damping was provided on the tank wall opposite the object in an effort to reduce acoustic standing waves in the tank.

C. EXPERIMENTAL PROCEDURE

The holography system was initially aligned to meet the coherence length requirement by altering the positions of the beam splitter and mirrors (Fig. 5) subject to the constraint that the undiverged reference beam and object-illuminating beam were centered on the plane of the photographic plate and the object respectively. Each mirror could be adjusted about its central axis to facilitate this operation. Minor adjustments were then made in the mirror's positions to make the two optical pathlengths as nearly equal as possible. Spatial filters, consisting of 25-micron-diameter pinholes which could be positioned at the focal point of a 10X microscope objective lens were next introduced into the beam paths as shown in Fig. 5. The spatial filters removed any light that was scattered or diverged from the laser beam and partially diverged the narrow beam. The intensity from a pinhole spatial filter has a Gaussian distribution with peak intensity at the center of the diverged beam [9]. Therefore, to illuminate the surface of the object and to provide the

portion of the reference beam incident on the photographic plate with approximately uniform intensity additional divergence of the beams was effected by using negative lenses after the spatial filters. These were kept clean and free from dust to minimize introducing scattered, incoherent light into the reference and object-illuminating beams.

The negative lenses were also selected to adjust the ratio of the intensity of the reference beam to the intensity of the object beam at the plane of the photographic plate. This ratio, of value 7.5:1, is optimal for KODAK Type 649F plates [4].

The system, after the above alignment, was used to produce holograms of objects either in air or submerged in water. When submerged objects were holographed, background noise was introduced into the beams by light scattering from small particles suspended in the water. Ideally, this could have been reduced by using a recirculating filter system on the water. Such a filter was not available. However, filtering the water on a single pass through an eighteen-inch column of fiberglass while filling the tank, and keeping the filled tank tightly covered against dust proved adequate to reduce the particle content so that holograms with good signal-to-noise ratios could be made.

The optimum exposure for Type 649F emulsion is 1100 ergs/cm^2 [2,4,8]. Exposure times for holographing submerged transducers were primarily dependent upon the amount of particulate matter suspended in the water. These exposure times

ranged from one to three minutes. Exposure times in air were usually on the order of thirty seconds.

During exposure the photographic plate was held rigidly in place by a specially-constructed stainless steel frame which fitted directly to the window frame on the outside of the tank. Care was exercised to allow each photographic plate to assume mechanical and thermal equilibrium before exposure.

The plates were developed in KODAK D-19 high-contrast developer. They were continually agitated during development to ensure uniform chemical action over the plate. After fixing, the plates were washed and then soaked in KODAK Photo-flo solution (a wetting agent), and the glass sides of the plates were wiped dry to aid in uniform drying of the emulsion.

The reconstructed virtual images were photographed with Polaroid Type 47 (ASA 3000) panchromatic film or a conventional panchromatic film when negatives were desired. Where the virtual image was approximately four feet from the holograph plane, a telescopic lens of fifteen-inch focal-length, was used on the camera to magnify the image.

IV. EXPERIMENTAL RESULTS

A. GENERAL RESULTS

The system was tested for its ability to construct time-averaged interferograms of acoustical transducers both in air and in water. While the system performed adequately for both mediums, certain limitations were recognized and difficulties encountered.

1. Mechanical Stability

The system was sufficiently stable to produce holograms both in air and in water for angles between the object and reference beams up to 30 degrees. Best results were achieved when these angles were 20 degrees or less. For angles beyond 30 degrees results were unsatisfactory. This was not considered to be a serious limitation since the geometry of the system and the sizes of the transducers examined did not require angles beyond 30 degrees.

2. Thermal Stability

This research was conducted from July through November. In the early months of the experiment the basement laboratory was relatively free of sudden temperature changes and the system performed satisfactorily. In the late fall and early winter months the laboratory was subject to temperature changes and air currents that seriously degraded the system and caused major power fluctuations in the laser's output. Toward the end of the experiment it was decided to

abandon the existing system and continue the experiment in a laboratory with a more stable thermal environment. Because of its size and weight the tank and its supporting base could not be relocated. Consequently, further efforts were conducted using a Gaertner-Jeong Holography System [4] and the Model 116 laser.

3. Other Limitations and Difficulties

The objects holographed in the designed system were approximately four feet distant from the photographic plate. While this in itself is not a problem, the moderate output power of the laser and the large solid angle through which the transducers' surfaces scattered the illuminating beam resulted in low intensity images in the holograms. The long time exposures placed strict mechanical and thermal stability requirements on the system. The illumination difficulty was partially overcome by painting the surfaces of the transducers with a translucent, glass-frosting paint or aluminum paint. The light scattered from the surfaces prepared in these ways was not randomly polarized but mostly retained the polarization of the illuminating beam. This technique provided more light to interfere with the reference beam than if the surfaces had been prepared with paint which polarized light randomly.

Additionally, the wavelength of the light source was not the best choice for attempting holography of transducers submerged in water. Red light is more highly attenuated by water compared to the blue-green light available from Argon-ion

lasers. However, the only available laser of sufficient power was the Model 116 and, while not an optimum choice, it did produce adequate results through a water medium.

Photographing the reconstructed virtual image through the holograph placed a noise source between the virtual image and the focal plane of the camera. Light was scattered from the silver grains in the emulsion which caused some fogging of the photographed image. This was not a serious impairment when the holograms had good image intensity. Image intensity could be greatly improved by bleaching, but the bleaching process enhances the light scattering ability of the holograph so that no improvement in image quality was realized.

One minor difficulty was present in that no instruments were readily available that could measure the absolute intensity of the light at the plane of the photographic plate, or that could measure the relative intensities of the reference and object beams. Consequently, "optimum" exposure time and beam ratio were established by trial and error. This was a costly and less than satisfactory method.

B. LOUDSPEAKER INTERFEROGRAMS

A seven-inch permanent-magnetic loudspeaker was holographed while being driven sinusoidally at 4000 Hz and 8000 Hz. The speaker was mounted in a 22" x 22" x 6" enclosure which was filled with sound-absorbing spun fiberglass. The speaker cone was painted silver to increase its reflectivity. Photographs of the interferograms are shown in Figs. 7 through 13.

1. Theory of Loudspeakers

At low frequencies where the wavelength of the sound is large compared to the radius of a speaker its cone may be assumed to move uniformly as a piston. Since the sound wave takes a finite time to propagate from the center of the cone to its rim, at high frequencies the cone's motion is no longer piston-like, but is similar to that of a vibrating membrane. The cone's motion may be "broken" into zones where some zones move outward while others move inward. The intensity of sound radiated by a speaker with such motion would be less than if the speaker moved as a piston. In order to reduce this effect, speaker manufacturers form concentric corrugations in speaker cones at some distance from the center which essentially "decouple" the inner portion of the cone from the outer portion when the speaker is driven at high frequencies [8].

A cross-sectional diagram of an idealized loudspeaker cone is shown in Fig. 6a. Concentric corrugations are shown at the rim and midway to the center of the cone. The cone may be thought to consist of inner and outer portions separated by the middle corrugations. Factors s_1 and s_2 correspond to the stiffnesses of the middle and outer corrugations respectively, while m_1 and m_2 denote the masses of the inner and outer portions of the cone. An idealized, lumped-parameter, mass-spring mechanical analog for the speaker cone is illustrated in Fig. 6b. An equivalent electrical-analog diagram is also shown in Fig. 6c. Here Lm_1, Lm_2, Cs_1, Cs_2, and

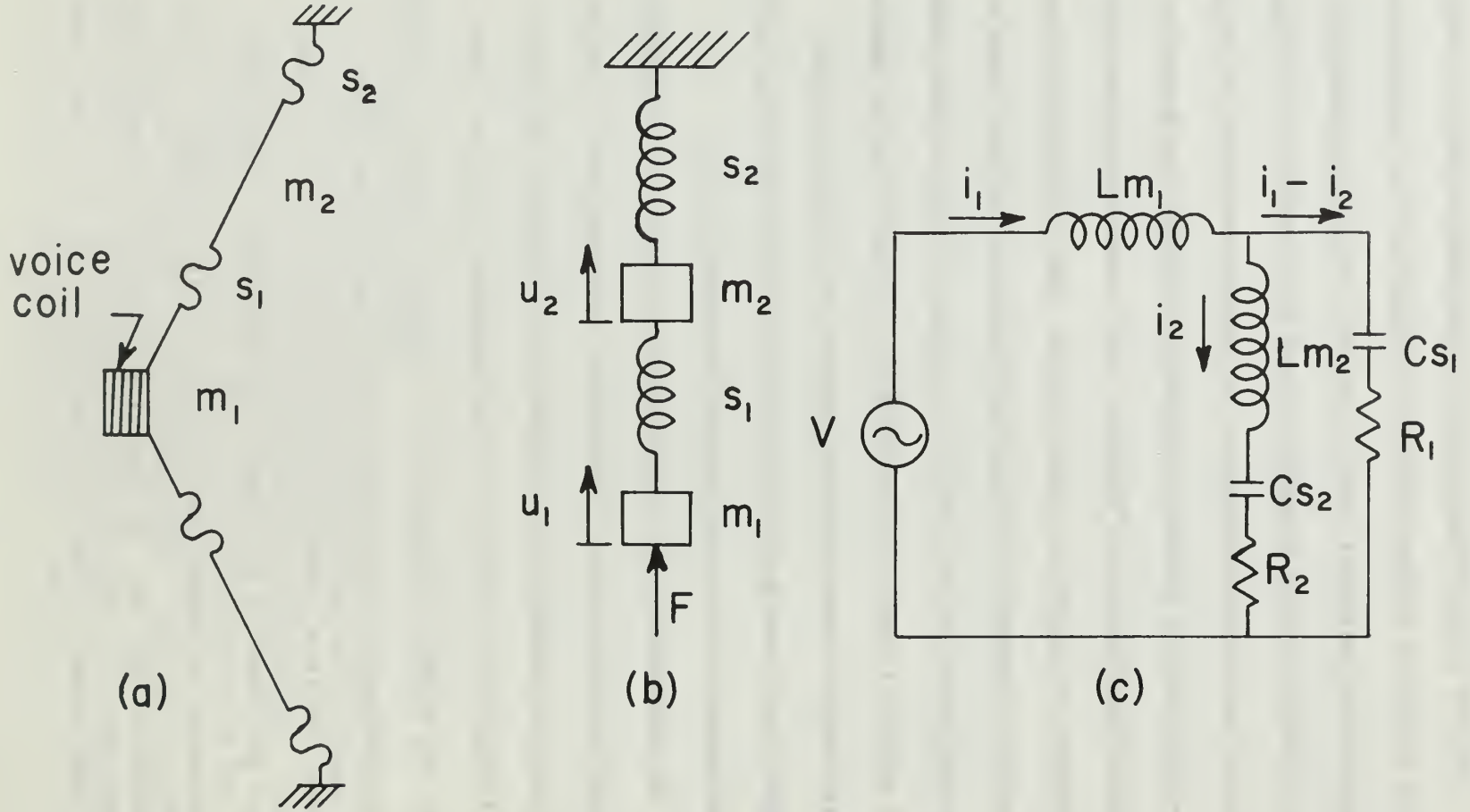

FIG. 6 SPEAKER CONE CROSS-SECTION and MECHANICAL and ELECTRICAL ANALOGS

the driving voltage V are proportional to m_1, m_2, s_1, s_2, and the driving force F respectively. The resistances R_1 and R_2 account for energy losses in the cone; these are due primarily to flexing at the corrugations [8]. Currents, i_1 and i_2 are proportional to the velocities u_1 and u_2 of the inner and outer portions of the cone. The capacitive reactances X_C associated with stiffnesses s_1 and s_2 are inversely proportional to frequency, while the inductive reactances X_L associated with masses m_1 and m_2 are directly proportional to frequency. Thus, at low frequencies the currents i_2 and i_1-i_2 are divided according to the ratio of the impedences of their respective branches. However, at high frequencies the reactance of Cs_1 becomes very small compared to that of the parallel branch; hence, i_2 becomes small compared to i_1. This is to say that at high frequencies the velocity of the outer portion of the cone is much less than that of the inner portion.

The axial sound pressure P generated by a piston mounted in an infinite baffle is [8]

$$P = \frac{\rho_0 c_0 k\pi a^2 U_0}{2\pi r} \qquad \text{IV.1}$$

where $\rho_0 c_0$ is the specific acoustic impedence of the medium, k the propagation constant, a the radius of the piston, r the distance from the piston along the longitudinal axis, and U_0 the velocity amplitude of the piston's face. Solving Eq. IV.1 for U_0 yields

$$U_0 = \frac{2Pr}{\rho_0 c_0 ka^2} . \qquad \text{IV.2}$$

If sinusoidal vibration is assumed, then

$$\xi = \frac{U_0}{\omega} \qquad \text{IV.3}$$

where ξ is the displacement amplitude of the piston's face, and $\omega = 2\pi f$ is the circular frequency. A combination of Eqs. IV.2 and 3 yields

$$\xi = \frac{2Pr}{\rho_0 c_0 ka^2 \omega} . \qquad \text{IV.4}$$

For a sound pressure level of 70dB re 0.0002 μbar at a distance of one meter on the axis, Eq. IV.4 predicts

$$\xi = \frac{0.14}{f^2} \text{ meters} \qquad \text{IV.5}$$

for radiation into air by a piston of 13.8 cm radius. If a speaker cone of the same size as that assumed for Eq. IV.5 has a complex motion which is assumed to be uniform with a superimposed standing-wave, then while the average displacement must be of the same order as that predicted by Eq. IV.5, in order that the same sound pressure level be radiated, some points of the speaker cone will be displaced distances greater than or less than the average. If these displacements are of sufficient amplitude, time-averaged interferograms of the speaker motion will display fringes corresponding to the peak displacements.

2. Interferograms

Figure 7 is a hologram of the stationary speaker. The varying intensity shown was a result of non-uniform scattering of light from the cone's surface. This was confirmed by viewing

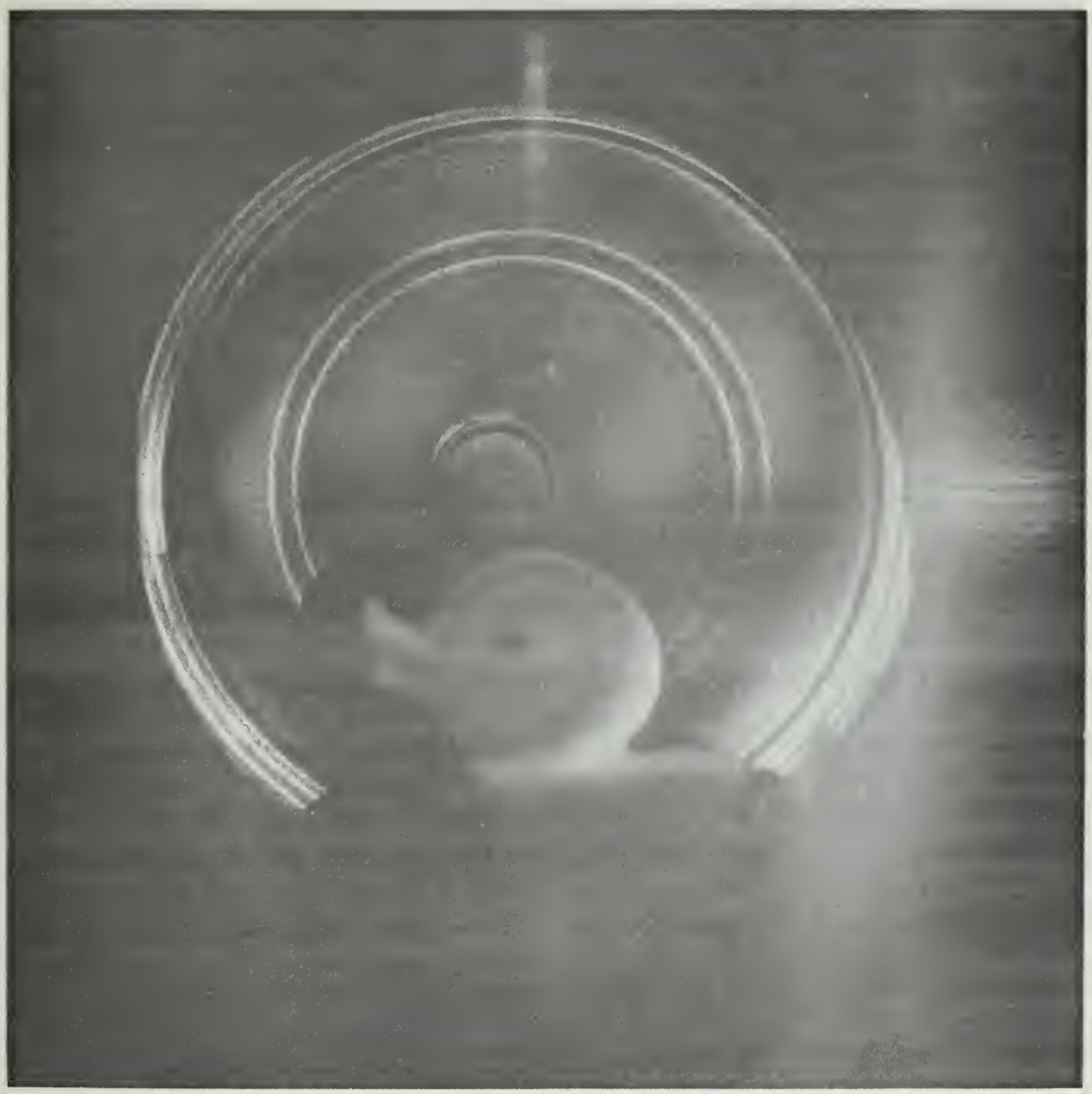

Figure 7. Reconstructed Hologram of a 7-inch Stationary Loudspeaker

the illuminated speaker with a polarizing filter, and the effect was minimized, but not wholly eliminated, in subsequent interferograms. This intensity variation might have been reduced further by painting the speaker cone with flat white paint, but this would have reduced the overall intensity. Corrugations in the speaker cone appear as two bright, concentric rings at approximately two-thirds the radial distance to the rim. A second set of corrugations is directly adjacent to the rim.

Figures 8, 9 and 10 are reconstructed interferograms of the 7-inch loudspeaker excited at 4000 Hz. The measured sound pressure level at one meter was increased 3dB after each interferograph. Increasing uniform motion caused the overall intensity of the interferograms to progressively decrease as would be expected from Eq. II.27. Generally, the same standing-wave pattern is recognizable in all the interferograms. First-order dark fringes are present in Fig. 8. These are most clearly seen in the lower-right quadrant of the speaker cone's inner portion. First-order dark fringes are also present in Fig. 9 in the same areas. A second-order, or nearly second-order, dark fringe appears in the lower-left quadrant of Fig. 9. First-order and second-order dark fringes are also evident in Fig. 10.

The angles $\emptyset_1$ and $\emptyset_2$ in the argument of Eq. II.27 were measured to be approximately 10° and 20° respectively for this sequence. For these angles Eq. II.27 predicts displacements at first-order and second-order dark fringes of

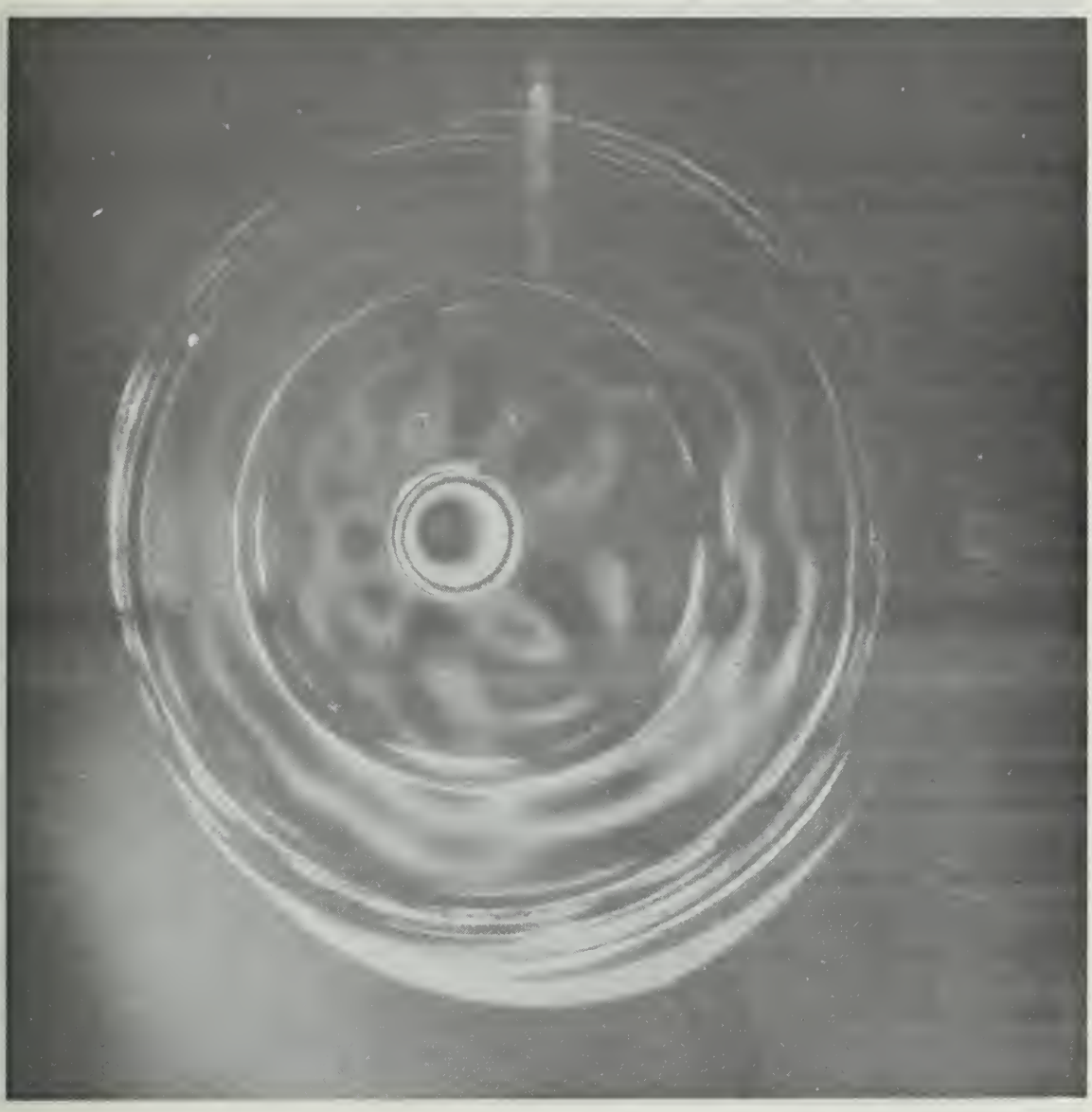

Figure 8. Reconstructed Interferogram of a 7-inch Loudspeaker

Frequency	4 kHz
Voltage to voice coil	0.3V p-p
SPL at 1 meter re 0.0002 microbar	72.8dB

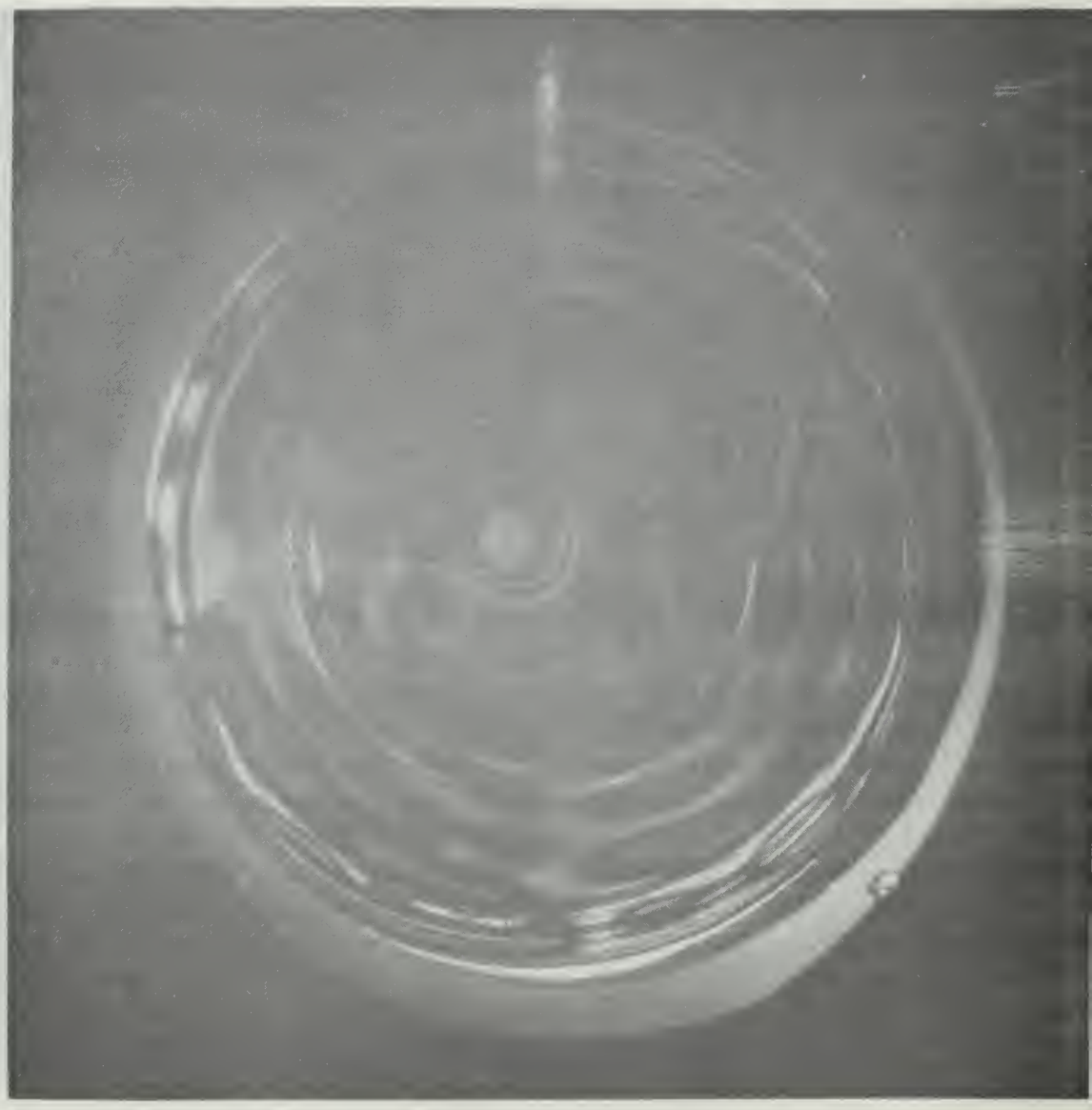

Figure 9. Reconstructed Interferogram of a 7-inch Loudspeaker

Frequency	4 kHz
Voltage to voice coil	0.42V p-p
SPL at 1 meter re 0.0002 microbar	75.8dB

Figure 10. Reconstructed Interferogram of a 7-inch Loudspeaker

Frequency	4 kHz
Voltage to voice coil	0.6V p-p
SPL at 1 meter re 0.0002 microbar	78.8dB

0.12 microns and 0.25 microns while Eq. IV.5 predicts an average displacement on the order of 0.001 microns at 4000 Hz. At first glance there seems to be a large disagreement between these predictions. However, only a part of the cone attained the peak displacements and closer examination of the sequence suggests that the cone was "broken up" into zones separated by nodes so that adjacent zones would move out of phase with each other. Thus, the average displacement would be only a small fraction of the peak displacement. While these peak displacements are contrary to any intuitive estimate of what they should be there does not appear to be any errors in the calculated peak or average displacements.

The speaker was mass loaded at four points by gluing four pennies to the speaker cone. This was done in an effort to cause the relative displacement from point to point to be increased compared to that of the unloaded cone. The resulting interferogram is shown in Fig. 11. Loading the cone achieved the desired effect. First-order and second-order dark fringes are evident in all quadrants of the speaker cone, and, of particular interest, the corrugations did not greatly impede the establishment of standing waves. This is also apparent in the unloaded cone sequence shown in Figs. 8, 9, and 10 but not as clearly as indicated in Fig. 11.

Figures 12 and 13 show reconstructed interferograms of the speaker driven at 8 kHz. The two cases differed by 3dB in axial sound pressure level measured one meter from the

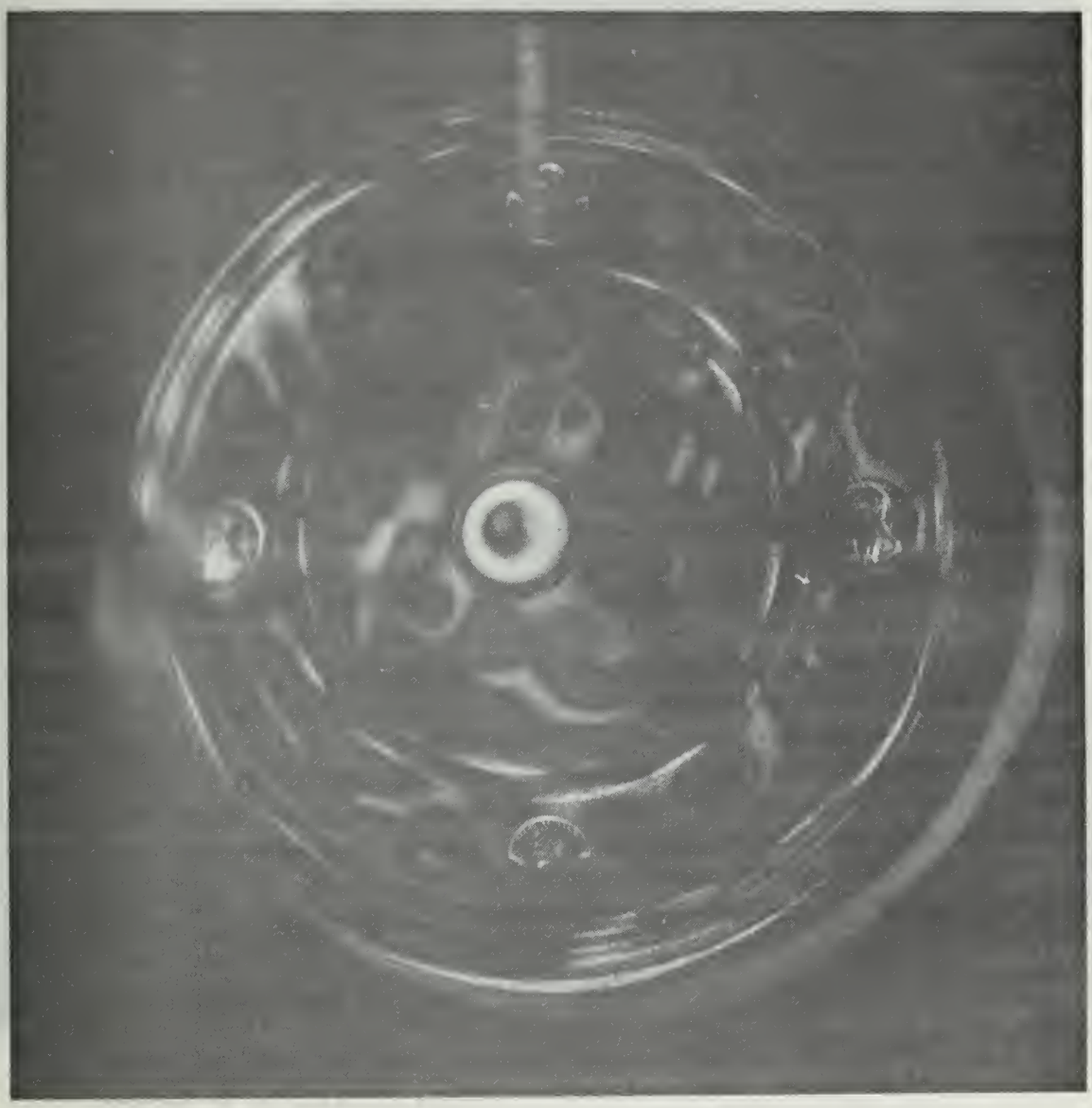

Figure 11. Reconstructed Interferogram of a Mass Loaded 7-inch Speaker

Frequency	4 kHz
Voltage to voice coil	0.42V p-p

Figure 12. Reconstructed Interferogram of a 7-inch Loudspeaker

Frequency	8 kHz
Voltage to voice coil	0.8V p-p
SPL at 1 meter re 0.0002 microbar	72.0 dB

Figure 13. Reconstructed Interferogram of a 7-inch Speaker

Frequency	8 kHz
Voltage to voice coil	1.2V p-p
SPL at 1 meter re 0.0002 microbar	74.7 dB

speaker. As in the sequence of interferograms shown in Figs. 8, 9 and 10 the two figures show essentially the same standing-wave pattern. The average displacement of the speaker cone shown in Fig. 13 is greater than that of the speaker cone shown in Fig. 12, thus, the overall decrease in intensity of the image in Fig. 13. Here too, the central corrugations do not appear to impede the generation of standing-waves. First-order dark fringes do not appear to have occurred except possibly near the center of the cone in Fig. 13. Since displacement is inversely proportional to frequency it would be expected that the displacements at 8 kHz would be less than at 4 kHz resulting in lower order fringing for Figs. 12 and 13.

V. CONCLUSIONS

The experiment conducted indicated that time-averaged holographic interferometry is a useful technique for analysis of sinusoidally-excited acoustic transducers provided the transducers are capable of generating sufficient power to produce large enough displacements for fringes to occur in the reconstructed interferogram. Unfortunately, this places a limitation on the application of holographic interferometry to analysis of those underwater transducers which can generate high sound pressure levels. However, except for the increased background noise present from light scatter in water, the technique can be employed with equal success for objects in air or submerged.

Successful operation of the experimental system indicated that holography and holographic interferometry can be pursued with adequate results provided attention is given to mechanical and thermal stability in the system; the coherence length of the light source is sufficiently long to provide depth of field; the optical path lengths are matched, and moderate care is exercised when processing and handling the holographs.

Interferograms of a sinusoidally-excited loudspeaker showed the standing-wave modes generated in the speaker cone. The interferograms indicated peak displacements much greater than an assumed average displacement.

VI. RECOMMENDATIONS

The existing holograph recording system, while adequate, would benefit from some improvements. Primary among these is that the system must be insulated against the temperature variations and air currents experienced in the laboratory.

Other improvements which would render the system more versatile are: (1) a High power laser, preferably of the Argon-ion gas discharge type, would enhance the hologram image intensity while the blue-green light of the Argon-ion laser would be less attenuated by water than the red light of a He-Ne laser. The Argon-ion laser has an inherent advantage over the He-Ne laser in that, in single mode operation, its coherence length is on the order of ten meters. (2) A film holder should be designed with micrometer adjustments in all degrees of freedom to facilitate repositioning holographs for real-time interferometry. (3) An instrument capable of measuring absolute light intensities should be procured to optimize the reference beam to object beam ratio and to accurately calculate exposure times. (4) Finally, if the system is to be used for holography of submerged objects the water tank should be equipped with a recirculating filter to reduce the particle content of the water.

BIBLIOGRAPHY

1. Stroke, G.W., An Introduction to Coherent Optics and Holography, p. 106-108, 137-138, Academe Press 1966.

2. Eastman Kodak Company, Kodak Plates and Films for Science and Industry, p. 4-5, 1962.

3. E.J. Feleppa, "Biomedical Applications of Holography," Physics Today, v. 22 no. 7, p. 25-26, July 1969.

4. Jeong, T.H., Gaertner-Jeong Holography Manual, p. 28, Gaertner Scientific Corporation, 1968.

5. Johnson, C.D., and Mayer, G.M., "Hologram Interferomtery as a Practical Vibration Measurement Technique."

6. Underwater Sound Laboratory Report 954, Stroboscopic Holographic Interferometery, by P. Shajenko and C.D. Johnson, 20 Sept. 1968.

7. Private communication - Mr. Reed Farrar, NOL, China Lake, California.

8. Kinsler, L.E., and Frey, A.R., Fundamentals of Acoustics, 2d.ed., p. 168, 248, 260-261, John Wiley and Sons Inc., 1962.

9. Naval Electronics Laboratory Center Technical Document 47, Holography Manual, by P.G. Lingenfielder, p. 26, Jan. 1969.

INITIAL DISTRIBUTION LIST

		No. Copies
1.	Defense Documentation Center Cameron Station Alexandria, Virginia 22314	20
2.	Library, Code 0212 Naval Postgraduate School Monterey, California 93940	2
3.	Commander, Naval Ordnance Systems Command Hqs. Department of the Navy Washington, D.C. 20360	1
4.	Associate Professor A.B. Coppens, Code 61Cz Department of Physics Naval Postgraduate School Monterey, California 93940	9
5.	LT David J. Griffiths 1716 Penn Avenue Scranton, Pennsylvania 18504	1

Unclassified
Security Classification

DOCUMENT CONTROL DATA - R & D

(Security classification of title, body of abstract and indexing annotation must be entered when the overall report is classified)

1. ORIGINATING ACTIVITY *(Corporate author)*
Naval Postgraduate School
Monterey, California 93940

2a. REPORT SECURITY CLASSIFICATION
Unclassified

2b. GROUP

3 REPORT TITLE
Application of Holographic Interferometry to Analysis of Sinusoidally-excited Acoustic Transducers

4. DESCRIPTIVE NOTES *(Type of report and inclusive dates)*
Master's Thesis; December 1969

5. AUTHOR(S) *(First name, middle initial, last name)*
David J. Griffiths

6. REPORT DATE	7a. TOTAL NO. OF PAGES	7b. NO. OF REFS
December 1969	52	9

8a. CONTRACT OR GRANT NO.	9a. ORIGINATOR'S REPORT NUMBER(S)
b. PROJECT NO. N/A	N/A
c.	9b. OTHER REPORT NO(S) *(Any other numbers that may be assigned this report)*
d.	N/A

10. DISTRIBUTION STATEMENT
This document has been approved for public release and sale; its distribution is unlimited.

11. SUPPLEMENTARY NOTES	12. SPONSORING MILITARY ACTIVITY
N/A	Naval Postgraduate School Monterey, California 93940

13. ABSTRACT

An application of optical holography known as "Holographic Interferometry" has been developed which enables experimentalists either to measure deformations of a few microns in loaded mechanical systems or to examine relative displacements in sinusoidally-vibrating systems. The fundamental theory of holography and four techniques for holographic interferometry are described in this report. A system constructed to record interferograms of acoustic transducers operating either in air or submerged in water is discussed and some results of examining a sinusoidally-excited 7-inch permanent-magnet loudspeaker with interferograms are considered.

DD FORM 1 NOV 65 1473 (PAGE 1)
S/N 0101-807-6811

14. KEY WORDS	LINK A		LINK B		LINK C	
	ROLE	WT	ROLE	WT	ROLE	WT
Holographic Interferometry						
Acoustic Loudspeaker						